Cracking in asphalt concrete

S.M.J.G. Erkens and J. Moraal
Road & Railroad Research Laboratory, faculty of Civil Engineering,
Delft University of Technology

Fatigue resistance of asphalt concrete is usually evaluated by means of fatigue tests, like repeated load four point bending tests. These tests are rather time consuming and, therefore, not suited for performance based specifications. In this article a new, faster procedure to determine the fatigue characteristics is introduced. The procedure is based on a combination of theory and experiments. Both the theorectical background and the experiments that were used are discussed in this article. Furthermore, fatigue relations that were developed using the new procedure and relations developped using classical fatigue tests, are compared.

keywords: **fatigue cracking, asphalt concrete, fracture mechanics, frequency sweep tests, direct tensile tests, stress intensity factor**

1 Introduction

Traffic loads are repetitive in nature and, therefore, lead to fatigue in the bound layers of the pavement structure. As a result, one of the design criteria for asphalt concrete roads is fatigue cracking. Fatigue cracks can initiate both at the top and at the bottom of a pavement. Cracks that initiate at the top are due to the outward shear stresses caused by the tyres. They are influenced by the characteristics of the wearing course (stiffness, roughness), but not by the pavement structure. Fatigue cracks that initiate at the bottom are caused by repetitive tensile stresses, which are the result of bending of the pavement layers due to passing wheel loads. This means they depent on layer thickness and stiffness. Therefore, these fatigue cracks are used as design criterion in the thickness design guide of the Dutch Ministry of Transport (RWS 1991). This criterion is based on the strain at the bottom of the pavement, due to a static standard axle load of 50 kN. This strain is determined by means of a linearly elastic multi-layer analysis of the pavement. The assumption of linear elasticity, however, is a crude simplification of the real material behaviour. In reality asphalt is an elasto-visco-plastic material (Figure 1). Since the material is also temperature dependant, the behaviour of asphalt is hard to model, especially without sophisticated test set-ups and powerful computers. Although, in the past years asphalt concrete research has been aimed at developing more sophisticated material models, this has not yet resulted in new design procedures.

In the design guide (RWS 1991), the relation between the above mentioned strain at the bottom of the asphalt pavement and the fatigue life time, defined as the number of load repetitions until the bending stiffness is reduced by fifty percent, is based on four point bending tests. These tests are rather time consuming, because they are based on the simulation of a large number of load

repetitions. Therefore, they are not suited for short term practical purposes like quality control. Until now, mix specifications are recipe-based, but modern construction contracts need to set specifications for the performance of the pavement in terms of cracking and permanent deformations. Obviously, the necessary back-up for these new, performance based, specifications will require a more simple and faster method to determine the fatigue characteristics of asphalt concrete.

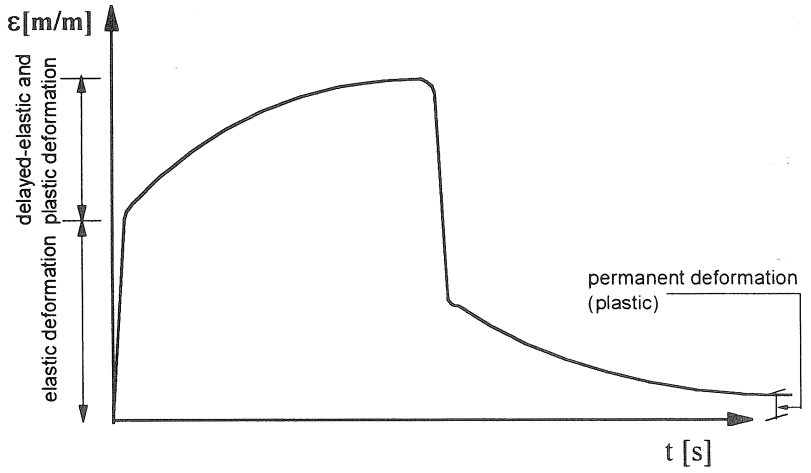

Fig. 1. Material behaviour of asphalt concrete.

2 Fatigue cracking, an overview

A crack is a discontinuity that both causes, and is caused by, stress concentrations. Due to flaws in the material at micro level (e.g. borders of the crystalline structure in metals or pores in (asphalt) concrete), stress peaks occur. In a plastic material such as steel, this will cause yielding at the stress tip, if the yield stress is reached. The material in the plastic zone will yield until it reaches its level of maximum deformation. After that, cracking occurs and the crack propagates. During the cracking process, three stages can be defined (Figure 2).

The first stage concerns the beginning of the fatigue process, in which the plastic zone in front of the crack tip is of the order of magnitude of the grain size. As a result, crack propagation in this stage is influenced by the microscopic structure of the material. In the second stage the plastic zone is much larger than the grain size, but smaller than the crack itself. In this stage Linear Elastic Fracture Mechanics (LEFM) can be applied. The third stage covers high stress levels and large plastic zones. The LEFM-theory can no longer be used, due to the large plastic deformations (Wei Wang 1991, Jacobs 1995).

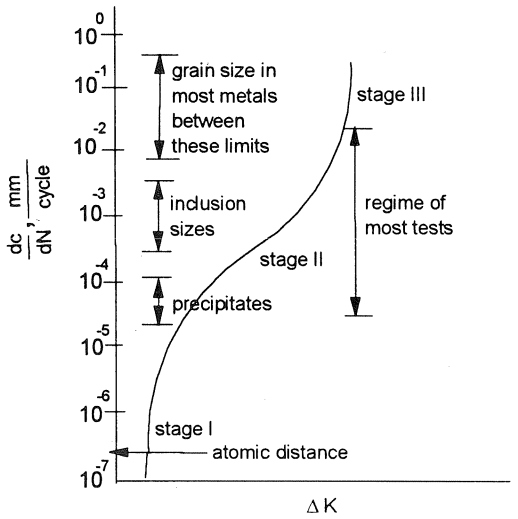

Fig. 2. Three stages in cracking (Wei Wang 1991).

The second stage can be described by Paris' law (1963):

$$\frac{dc}{dN} = A(\Delta K)^n \tag{1}$$

Where

c = crack length
N = number of load repetitions
A, n = material parameters
ΔK = $K_{max} - K_{min}$ = difference between the minimum and maximum stress intensity factor during cyclic loading. For a full sine load, K_{min} is zero (under compression).

In semi-brittle materials like (asphalt) concrete, the plastic deformations at the crack tip are negligible. Instead, a "process zone" of micro cracks exists in front of a macro crack. In the process zone the material is softening (there remains some tensile strength), while the macro crack has zero tensile strength. When the part of the process zone next to the crack tip reaches zero tensile strength, the crack propagates, causing new micro cracks at the opposite end of the process zone due to stress redistribution (Figure 3).
Based on the crack tip model shown in Figure 4 Schapery (1975) developed a theory to describe the time-dependent size and shape of cracks in linearly visco-elastic, isotropic media. For these media he established, among others, that Paris' law could be used to describe the crack growth and that the parameters depend on the material characteristics mentioned in Equation (2).

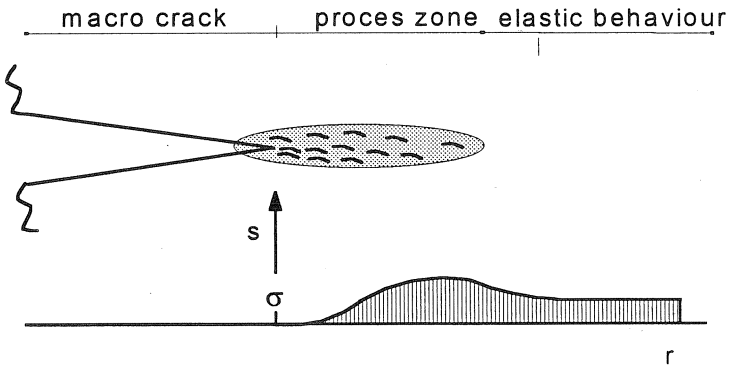

Fig. 3. Cracking in semi-brittle materials involves a process zone where micro cracks occur (showing the stress (σ) at a distance r from the crack tip).

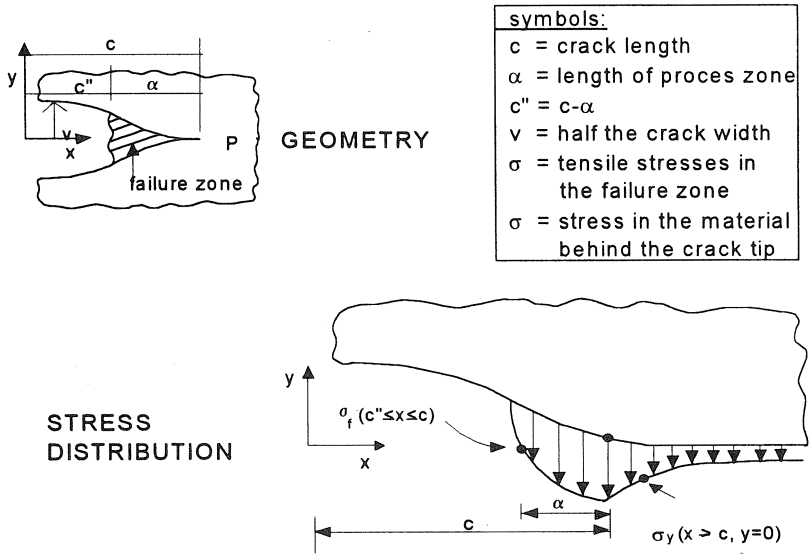

Fig. 4. Crack-tip model for brittle cracking, used by Schapery (Barenblatt 1962).

$$n = \frac{2}{m} \text{ and } A = \frac{\pi}{6 f_t^2 I_1^2} \left(\frac{(1-\nu^2) D_2}{2\Gamma} \right)^{\frac{1}{m}} \left| \int_0^{\Delta t} w(t)^{2(1+\frac{1}{m})} \, dt \right| \quad (2)$$

with:

$$m = \frac{d \log(S_{mix})}{d \log(T_{load})}$$

$$\log(S_{mix}) = a_0 + a_1 \log(T_{load})$$

(T_{load}) = loading time

f_t = tensile strength

I_1 = $\frac{\pi K_1}{2\alpha\sigma}$, integration of the stresses at the cracktip over length of the failure zone (α)

K_1 = stress intensity factor for mode *I* loading

α = size of the plastic zone in front of the crack tip

v = Poisson's ratio

D_2 = $\frac{1}{S_{mix}(\log(T_{load}) = 0)}$

Γ = fracture energy

$W(t)$ = pulce shape of the stress intensity factor related to time

The above mentioned expressions for A and n were related to an ideal linear visco-elastic, isotropic material. However asphalt concrete is not an ideal material, it is heterogeneous, non-isotropic and it contains voids. Furthermore, Schapery's expressions are based on a linear relation between the mix stiffness (S_{mix}) and the loading time (T_{load}) on a double logarithmic scale, while Jacobs' experiments (1995) showed that for asphalt concrete this should be a second order polynomial. Therefore, these expressions had to be adapted to describe crack growth in asphalt. This was done by Jacobs and extended to Gravel Asphalt Concrete by Erkens et al. (1995). Jacobs showed that Schapery's expression for n could be used if a correction factor was applied. This correction factor covered the influence of the air voids and the deviation between Schapery's linear $S_{mix} - T_{load}$ relation and his parabolic one. For the formulation of A, Jacobs used all the material parameters used in Schapery's equation, with the exception of υ (Poissons ratio). Based on these material characteristics he established a regression relation for A. This resulted in the following equations:

$$n = \frac{2}{m \cdot CF} \text{ and } \log(A) = d - 2a \cdot \log(f_t) - b \cdot \frac{n}{2} \cdot \log(2\Gamma) - c \cdot \frac{n}{2} \cdot \log(S_{mix}) \qquad (3)$$

with:

$$m = \frac{d\log(S_{mix})}{d\log(T_{load})}$$

S_{mix} = $a_0 + a_1 \cdot \log(T_{load}) + a_2 \cdot (\log(T_{load}))^2$

S_{bit} = bitumen stiffness

$\log(CF)$ = $-1.1524 + 0.6016 \cdot \log(V_a) + 0.5958 \cdot \log(S_{bit})$

f_t = tensile strength

Γ = fracture energy

V_a = volume percentage air voids, in %

a_i, b, c, d = regression constants

Since, the above mentioned parameters (e.g. tensile strength) can be determined by means of non-fatigue tests, the time necessary to determine fatigue characteristics can be reduced. In the next

section a method to determine the fatigue characteristics of specimens taken from a road or test section is discussed. Such a method can be extremely useful for short term practical purposes like quality control.

3 A new procedure to determine the fatigue characteristics of asphalt concrete

Specimen preparation

In order to keep the procedure useful for practical purposes, obtaining and preparing the specimens must be simple as well. Since the current standards are based on fatigue cracks that initiate at the bottom, it is the bottom layer of the pavement from which the fatigue characteristics should be determined. In Dutch roads this bottom layer usually consists of Gravel Asphalt Concrete (GAC) and therefore, this was the material considered in the project. The specimens were obtained according to the method developed at the Texas A&M University during the SHRP A005 project (Lytton et al. 1993): a 150 mm diameter core is drilled from a road. At the top of each core an arrow was drawn to indicate the traffic direction. The actual specimens are then drilled from the bottom layer of these cores, perpendicular to the traffic direction (Figure 5). These specimens have a rounded top and bottom side, and a maximum height of 150 mm. Based on considerations concerning the required dimensions and the maximum aggregate size, the diameter of the specimens is fixed at 75 mm.

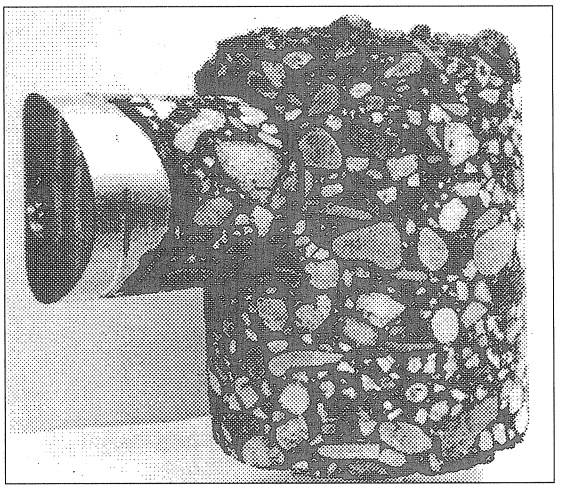

Fig. 5. The 75 mm diameter specimens are drilled out of 150 mm diameter samples (the sample is placed up-side down in this picture).

The next step in specimen preparation is the gluing of the end-caps. It is important that the caps are placed concentrically, because a non-concentric placement of the caps results in a reduction of the contact surface that is used for load transfer. As a result, the contact stresses increase, which causes failure at the end-caps rather than in the middle part of the specimen. To ensure that the

caps are placed exactly concentric and to make gluing easier, a gluing mould has been used (Figure 6).

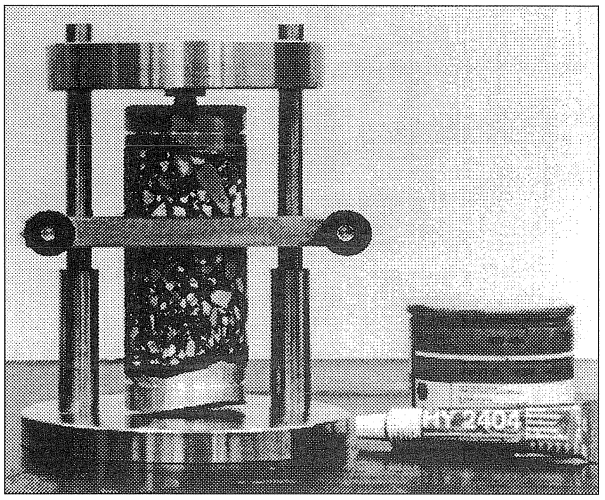

Fig. 6. A gluing mould was used to position the end-caps concentrically.

Frequency sweep tests

To determine the mix stiffness (S_{mix}) and the variation of S_{mix} as a function of the loading time, the frequency sweep test was used. This is an uniaxial dynamic test in which the specimens are subjected to a fully reversed sinusoidal load with an amplitude of 10 to 20% of the expected tensile strength of the specimens. The choice for a fully reversed load is due to the observations of a considerable amount of creep for pure tension tests. The maximum stress is kept low to prevent damage to the specimens. The frequency sweep tests are performed at five different temperatures (5, 15, 20, 25 and 35°C). At each temperature level seven loading frequencies are applied (0.5, 1, 2, 4, 8, 16 and 25Hz). The deformation of the specimens for every combination of temperature and loading frequency is measured by two LVDT's, placed opposite to each other on the specimens (Figure 7).

From the average deformation measured by the two LVDT's and the applied force, the mix stiffness was computed. The method suggested by Jacobs (1991) was used to correct this stiffness for the influence of the weight of the parts connected to the specimen. For each specimen, the dynamic test results in a diagram showing S_{mix} as a function of loading time (defined as $T_{load}=f^{-1}$) and temperature (Figure 8). From this diagram, a mix stiffness mastercurve can be constructed (Van der Poel 1955). In this curve the mix stiffness is expressed as a function of the mastercurve loading time, which is a function of the applied loading time and the test temperature (Van der Poel 1955). The mastercurve is related to a reference temperature, in this case 20°C, and the results obtained at other test temperatures are horizontally shifted to a new loading time (Erkens et al. 1995). The mix stiffness at this new loading time and the reference temperature is the same as the mix stiffness under the actual test conditions.

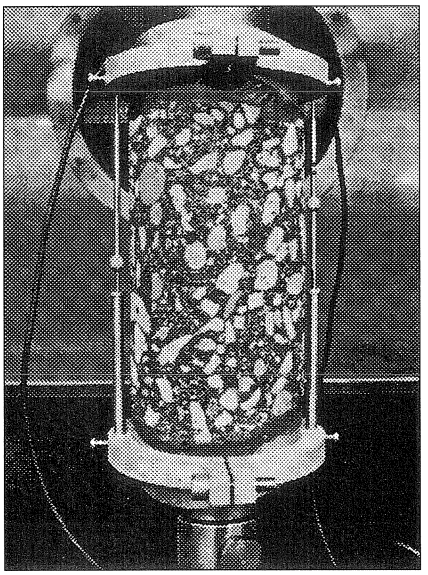

Fig. 7. A specimen with two LVDT's connected to it.

Thus, the data points are shifted to construct a mastercurve, through which a second order polynomial is fitted. This polynomial can be used to determine both the mix stiffness and its variation as a function of the loading time and temperature (= T_{mas}) for the complete range of test conditions. This means that two of the material characteristics that are needed to determine the parameters from Paris' law, mix stiffness and mix stiffness variation, are available.

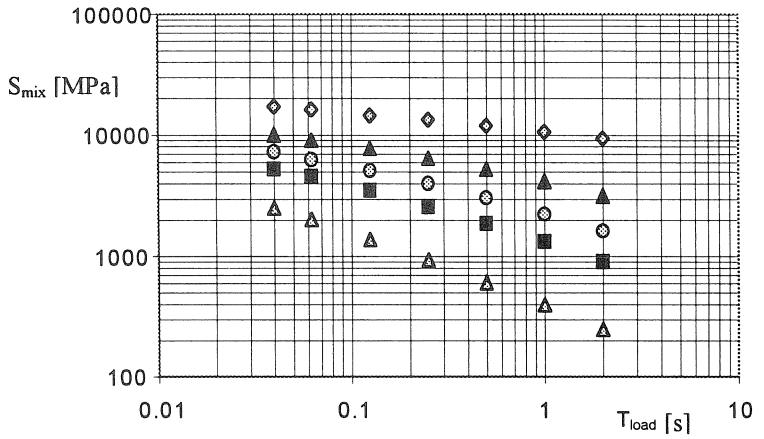

Fig. 8. Results from the frequency sweep test at five temperature levels.

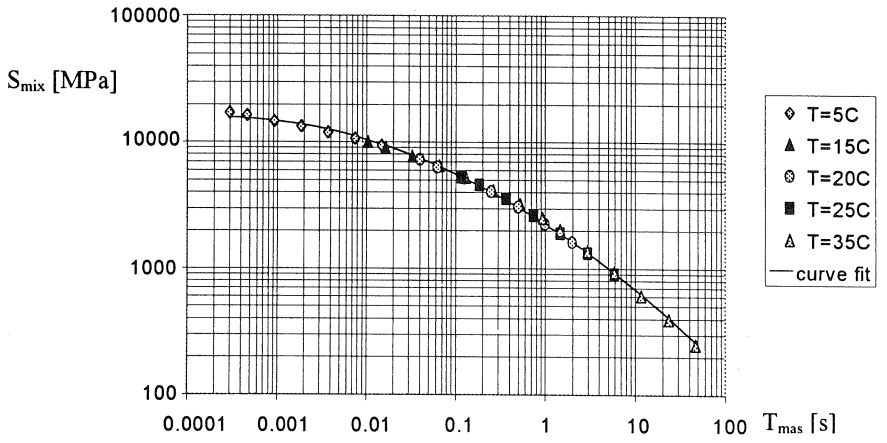

Fig. 9. Mix stiffness mastercurve with reference temperature T = 20° C.

Direct tensile tests

After completing the frequency sweep test series, the necessary parameters concerning the mix stiffness are known. What remains to be determined are the tensile strength and the fracture energy. This information is determined by means of the direct tensile test, which is a destructive test in which the specimens are subjected to a continuous deformation rate of 0.425 mm/s at a temperature of 20°C (Figure 10).The displacement rate is chosen rather arbitrary. The total displacement and the force necessary to induce that displacement are measured by means of the equipment's internal LVDT and its loadcell, respectively.

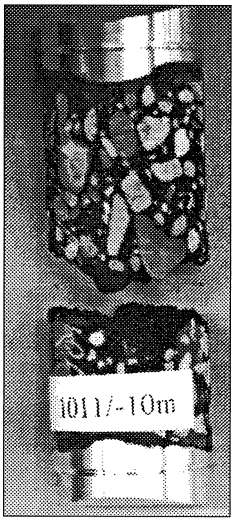

Fig. 10. A specimen after the (destructive) direct tensile test.

This test results in a force-displacement diagram for each specimen (Figure 11). From this diagram the tensile strength can be obtained by dividing the maximum force by the specimens original cross section. For the fracture energy Jacobs (1995) used the area under the curve as an approximation. In the remainder of this article the term "fracture energy" will be used for this approximation.

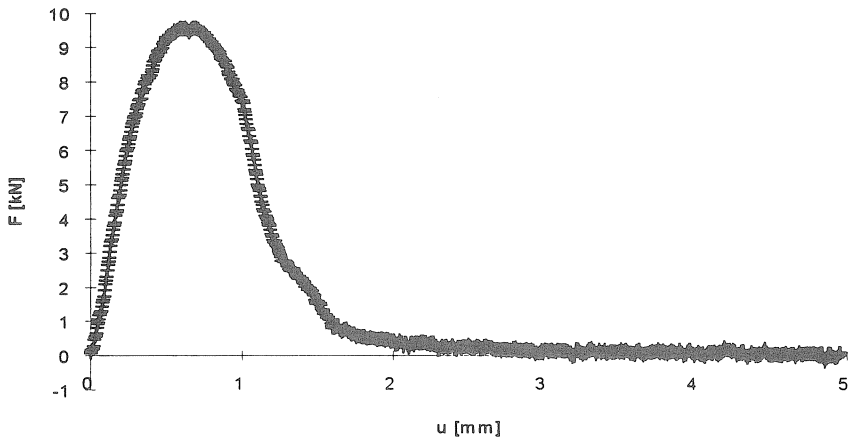

Fig. 11. The direct tensile test results in a load-displacement diagram for each specimen.

As stated at the beginning of this paper, asphalt concrete characteristics are temperature and loading time dependant. This is due to the bituminous binder. Since the influence of both time and temperature on the stiffness is well known, other characteristics are often expressed as a function of the stiffness (either bitumen stiffness or mix stiffness). In this way the effects of temperature and loading time are implicitly dealt with. Heukelom (1966), established a relation between the relative tensile strength of a mix and the corresponding bitumen stiffness (Figure 12). Jacobs (1995) developed a regression relation which was later on enhanced by Sabha et al. (1995). A similar relation for the relative fracture energy was developed by Jacobs. This relation has also been adapted by Sabha et al., in order to expand the range of bitumen stiffnesses for which the relation was valid.

In order to use these relations, the bitumen stiffness must be known. Since the resulting mix stiffness is a function of the bitumen stiffness and the mix composition, the S_{bit} can be computed based on the values of S_{mix} and the mix composition, using a relation developed by Francken (1977, 1995). For an extensive description of this procedure the reader is referred to Erkens et al. (1995) and Sabha et al. (1995). After the bitumen stiffness has been determined, the relative tensile strength and fracture energy can be computed by means of Equations (4) and (5).

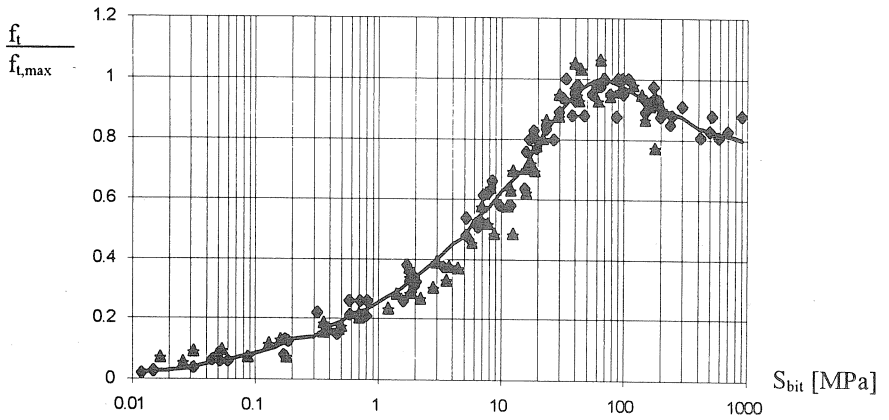

Fig. 12. Relation between the relative tensile strength and the bitumen stiffness.

$$\log\left(\frac{f_t}{f_{t,max}}\right) = -0.60174 + 0.44611\log(S_{bit}) - 0.03474\log^2(S_{bit}) - 0.02119\log^3(S_{bit}) \quad (4)$$

$$\log\left(\frac{\Gamma}{\Gamma_{max}}\right) = -0.131 + 0.501\log(S_{bit}) - 0.478\log^2(S_{bit}) \quad (5)$$

Jacobs (1995) showed that, by using these relations, the tensile strength and fracture energy from the direct tensile test can be related to any of the temperature and loading time combinations that are covered by the mix stiffness mastercurve.

When these material characteristics are substituted in Equation (3), the parameters from Paris' law are obtained. This means that two simple tests suffice to determine the fatigue characteristics of asphalt concrete.

4 Relating the new procedure to the current standard

As stated in the first part of this article, the objective of this project was twofold. The first objective, determining the parameters of Paris' law for asphalt concrete asphalt concrete by means of relatively simple tests, has been fulfilled in the previous section. In this section the second objective, relating these parameters to the fatigue model used in the current standard, will be treated. As discussed in the first section, the current specifications for fatigue are based on the four point bending test. The strain at the bottom side of the beam and the stiffness are used as input parameters to determine the number of load repetitions until failure. In order to come up with requirements for the Paris parameters of asphalt mixes, a relation between these parameters and the existing specifications is necessary. This meant, first of all, that Paris' law had to be rewritten:

$$\frac{dc}{dN} = AK^n \Leftrightarrow N = \int_{C_0}^{C_1} \frac{1}{AK^n}\, dc = h \int_{C_0/h}^{C_1/h} \frac{1}{AK^n}\, d\frac{c}{h} \tag{6}$$

Where

c_0 = crack length at the beginning of the test

c_1 = crack length at the end of the test

h = beam height

To solve this integral expression for N, an expression for K as a function of the relative crack length is necessary.

In the second section of this article it was shown that a process zone exists in front of a crack in (asphalt) concrete. Although the stress distribution in this zone is non-linear, LEFM can still be applied if the size of the process zone is small compared to the specimen size. Gettu et al. (1991) stated that, due to the presence of a sizeable fracture proces zone in cement-based composites, LEFM cannot be applied to describe fracture in these materials. For concrete several models have been developed to describe the discontinuous, non-linear processes that take place in this zone. These models can be divided into two categories, cohesive and effective (or equivalent) crack models (Gettu et al. 1991). Since the cracking proces in asphalt concrete is similar to that in concrete, Jacobs adopted a concrete-like equivalent crack model (Scarpas et al. 1994). Such a model is based on the assumption of an equivalent crack, which causes the same damage as the physical crack. Unlike the physical crack, the equivalent crack's behaviour can be described by means of LEFM.

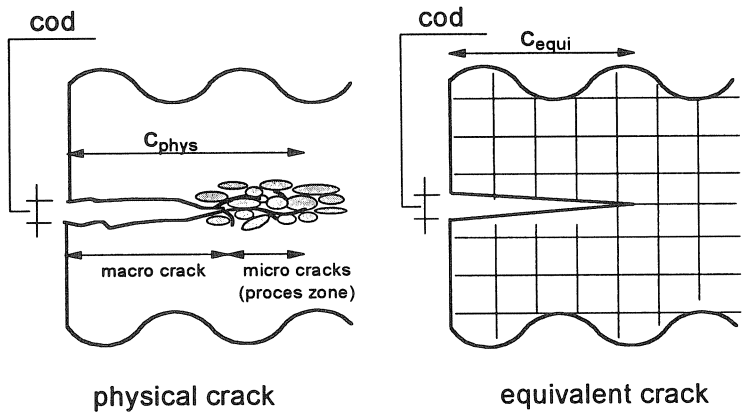

Fig. 13. Physical versus equivalent crack.

Jacobs used a finite elements simulation (Scarpas et al., 1993) of his direct tensile fatigue test in which the damage was concentrated in one discrete crack. The condition that the equivalent crack should cause the same damage as the physical one (crack + process zone) was fulfilled by demanding that the crack opening displacement (COD) due to the discrete crack had to be the same

as the COD due to the physical crack (Figure 13). This way, the non-linear processes in the process zone are taken into consideration without a model that identifies and quantifies them. Thus, based on his experimental *N* versus COD data, Jacobs obtained a diagram expressing *N* as a function of the equivalent crack length (Figure 14) (Scarpas et al. 1994).

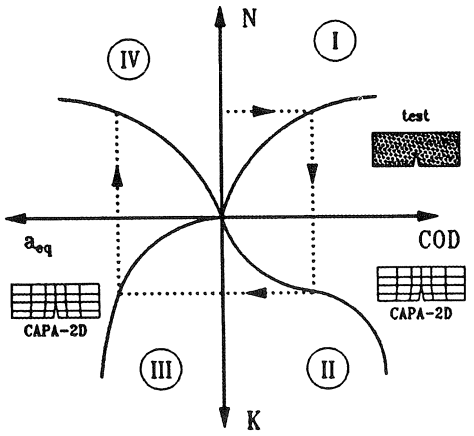

Fig. 14. Graphical presentation of the method used to relate the test results to Paris' law.

From the finite elements simulation of the test the stress intensity factor as a function of a_{eq} was obtained, using this the relation between *N* and *K* could be established. From this relation, Jacobs derived the expressions for *A* and *n* that are mentioned in Equation (3). So, these parameters are related to an equivalent crack. A similar approach was used to determine the stress intensity factor from a beam subjected to the four point bending test.

In a real four point bending test the beam is subjected to a full sine load, causing alternating tensile and compressive stresses in the top and bottom of the beam. As a result, a four point bending specimen is damaged both at its upper and lower part. For the finite element simulation this would mean two discrete cracks, one initiating at the top and growing down, while another one initiated at the bottom and grew up. But since there is no model to describe the behaviour of cracks in asphalt concrete under compression, a simulated crack would simply close under compression and transfer the compressive stresses. This means that a crack in the compressive zone doesn't influence the crack in the tensile zone. Therefore, a single crack was used in the numerical simulation. This resulted in a relation between the corresponding stress intensity factor and the relative crack length. When the results from the finite element analysis were compared to the results from an experimental project by Salam and Monismith (1972) who used specimens with a notch on one side to determine the stress intensity factor of a four point bending test, they showed a striking resemblance in the first (important) part of the curve (Figure 15). This indicates that the equivalent crack provides a good indication of the damage in the tensile zone.

The stress intensity factor is defined as:

$$K = \sigma\sqrt{c} \cdot \beta\left(\frac{c}{h}\right) \tag{7}$$

Where

σ = reference stress somewhere outside the crack zone
c = crack length
h = beam heigth
β = a test geometry dependant function that relates K to the reference stress

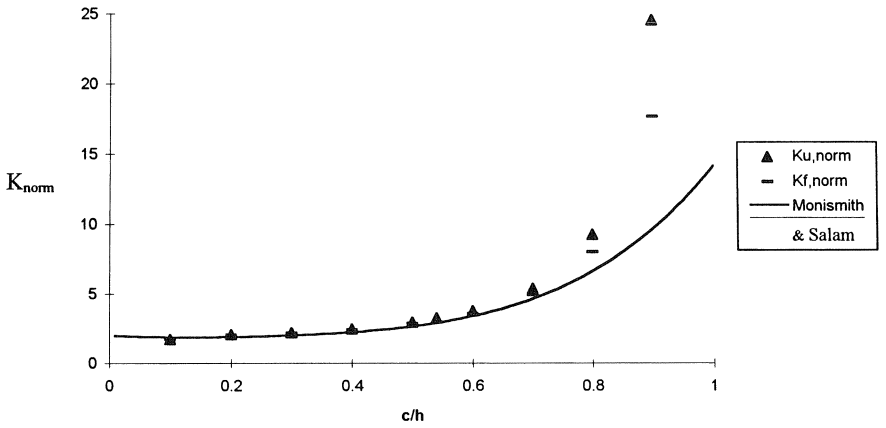

Fig. 15. The normalised K-values of both the displacement ($K_{u,\,norm}$) and the force controlled ($K_{f,norm}$) CAPA-simulation of the four point bending test can be described by the formulation of Monismith and Salam (1972) ($K_{norm} = K/(\sigma\sqrt{c}) = \beta(c/h)$).

The expression obtained by Salam and Monismith for the normalised stress intensity factor was:

$$\beta\left(\frac{c}{h}\right) = 1.99 - 2.47\left(\frac{c}{h}\right) + 12.97\left(\frac{c}{h}\right)^2 - 23.17\left(\frac{c}{h}\right)^3 + 24.8\left(\frac{c}{h}\right)^4 \tag{8}$$

Substituting (8) in (7) and using the stress in the bottom fibre of the beam before cracking as reference stress, the following expression is obtained:

$$K = \sigma\sqrt{c} \cdot \beta\left(\frac{c}{h}\right) \text{ and } \sigma = \frac{6Fs}{bh^2} \text{ (see Figure 16 for the meaning of the symbols).}$$

$$K = \frac{6Fs}{bh^2}\sqrt{c}\left\{1.99 - 2.47\left(\frac{c}{h}\right) + 12.97\left(\frac{c}{h}\right)^2 - 23.17\left(\frac{c}{h}\right)^3 + 24.8\left(\frac{c}{h}\right)^4\right\} \quad \Leftrightarrow$$

$$K = \frac{6Fs}{bh^{1.5}}\left\{1.99\left(\frac{c}{h}\right)^{0.5} - 2.47\left(\frac{c}{h}\right)^{1.5} + 12.97\left(\frac{c}{h}\right)^{2.5} - 23.17\left(\frac{c}{h}\right)^{3.5} + 24.8\left(\frac{c}{h}\right)^{4.5}\right\} \tag{9}$$

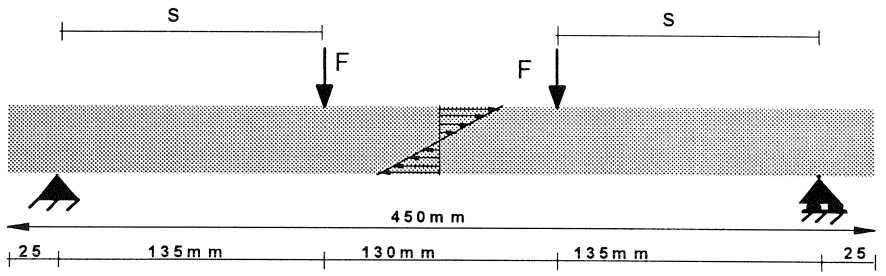

Fig. 16 Geometry of the four point bending test.

After substitution of (9) in (6) and some rearranging, the expression for N becomes:

$$N = \left\{ \frac{h^{(1-\frac{n}{2})}}{A[S_{mix}]^n} \int_{c0/h}^{c1/h} \frac{1}{\left[\left\{ 1.99\left(\frac{c}{h}\right)^{0.5} - 2.47\left(\frac{c}{h}\right)^{1.5} + 12.97\left(\frac{c}{h}\right)^{2.5} - 23.17\left(\frac{c}{h}\right)^{3.5} + 24.8\left(\frac{c}{h}\right)^{4.5} \right\} \right]^n} d\frac{c}{h} \right\} \cdot \varepsilon^{-n} \quad (10)$$

$$N = a\varepsilon^{b} \quad (11)$$

Expression (11) yields N-ε relations like those in the Dutch design guide (DWW 1991). The average result from the analysis performed in this project was compared to the mean fatigue line that was derived for Gravel Asphalt Concrete by means of four point bending (Figure 17). This comparison shows that the developed procedure is suitable to determine the fatigue characteristics of Gravel Asphalt Concrete quite accurately.

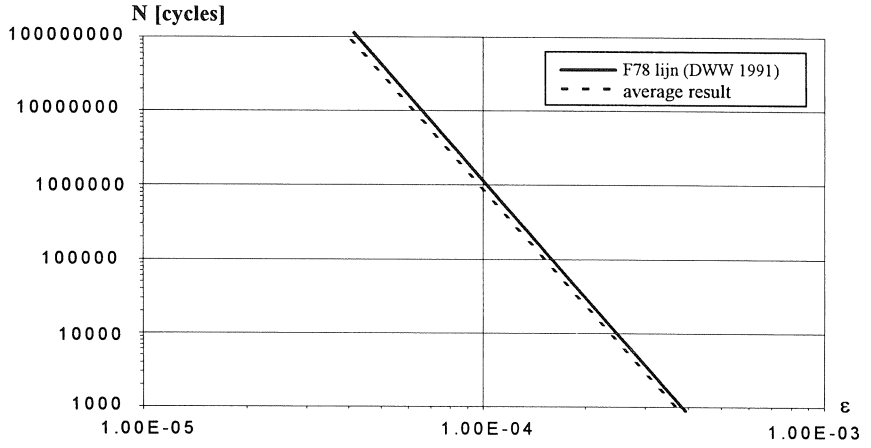

Fig. 17 The average result of the new procedure compared to the design line.

5 Conclusions

Although, the procedure still inhibits several simplifications of asphalt concrete material behaviour, it is believed that the fatigue characteristics of asphalt concrete can be determined effectively by means of frequency sweep and direct tensile tests. This eliminates the need to perform time consuming repeated load fatigue tests. Therefore, this procedure is especially useful for short-term practical purposes such as quality control.

List of symbols

LEFM	Linear Elastic Fracture Mechanics
GAC	Gravel Asphalt Concrete, asphalt mix that is often used for the bottom layer of a pavement
c	crack length [mm]
h	beam height
b	beam width
α	size of the plastic zone / process zone in front of the crack tip
ε	strain
υ	Poisson's constant
N	number of load repetitions until failure, fatigue life
A,n	parameters from Paris' law
Γ_{sch}	fracture energy, defined by Schapery
Γ	in the article this is referred to as "fracture energy", actually it is an approximation of the fracture energy, defined by Jacobs as twice the area under the load-displacement curve
Γ_{max}	maximum fracture energy
f_t	tensile strength
$f_{t,max}$	maximum tensile strength
σ_{ref}	reference stress, used in definition K, stress somewhere outside the crack zone
S_{mix}	mix stiffness, the stiffness of the asphalt concrete mixture
$S_{mix,\infty}$	maximum mix stiffness
S_{bit}	bitumen stiffness
$S_{bit,\infty}$	maximum bitumen stiffness, glass modulus ≈ 3000 MPa
ΔK	maximum stress intensity factor minus minimum stress intensity factor
K_{max}	maximum stress intensity factor
K_{min}	minimum stress intensity factor
K_1	stress intensity factor for mode I loading (opening mode)
T_{mas}	mastercurve loading time, a function of the actual loading time and the temperature
K_{norm}	normalised stress intensity factor = $K / \sigma_{ref}\sqrt{c} = \beta(c/h)$
$K_{u,norm}$	normalised stress intensity factor for a displacement controlled test
$K_{f,norm}$	normalised stress intensity factor for a force controlled test
V_g	volume percentage aggregate
V_b	volume percentage binder (=bitumen)

V_a volume percentage air voids

$w(t)$ pulse shape of the stress intensity factor related to time

m $\frac{d\log(S_{mix})}{d\log(T_{load})}$, slope of the mix stiffness master curve

I_1 $\frac{\pi K^1}{2\alpha\sigma}$, integration of the stresses at the cracktip over length of the failure zone (α)

References

BARENBLATT, G.I. (1962), "the Mathematical Theory of Equilibrium Cracks in Brittle Fracture", *Advances in Applied Mechanics,* Vol. VII, Academic Press

ERKENS, S.M.J.G. and MORAAL, J. (1995), "a Practical Method to Determine the Fatigue Characteristics of Asphalt Concrete", RRRL-report nr.7-95-117-1, ISSN 0169-9288, Delft University of Technology

FRANCKEN L. (1977), "Module Complexe des Mélanges Bitumineux", *Bull. Liaison Labo. P.et Ch. spécial V*

FRANCKEN L. (1995),"the Rheology of Bituminous Binders", *European Workshop-5th to* 7th April 1995, Paper No. 47

GETTU, R., OUYANG, C. and SHAH, S. (1991), "Fracture Mechanics of Concrete - a Review", *Proceedings of the International Symposium of Fatigue and Fracture in Steel and Concrete Structures,* Mardras, India, page 341-364

HEUKELOM, W. (1966), "Observations on the Rheology and Fracture of Bitumens and Asphalt Mixes", *AAPT,* Vol. 35 pages 358-399,

JACOBS M.M.J. (1991), "Cracking of Asphalt Concrete ", RRRL report nr. 7-9 111 6-6, ISSN 0169-9288, Delft University of Technology

JACOBS M.M.J. (1995), "Crack Growth in Asphaltic Mixes", Ph. D.Thesis, Delft University of Technology, NUGI 834,

LYTTON R.L., UZAN J., FERNANDO E.G., ROQUE R., HILTUNEN D. and STOFFELS S.M. (1993), "Asphalt Concrete Pavement Distress Prediction: Laboratory Testing, Analysis, Calibration and Validation", SHRP A005 report

NILSSON, R.N., OOST, I. and HOPMAN, P.C. (1996), "Visco-Elastic Analysis of Full Scale Pavements: Validation of VEROAD" in *proceedings Transportation Research Board* proceedings, Washington

PARIS P.C. and ERDOGAN F. (1963), "A Critical Analysis of Crack Propagation Laws", *Transactions of the ASME, Journal of Basic Engineering,* Series D, 85, No. 3

POEL, C. VAN DER (1955), "Time and Temperature Effects on the Deformation of Asphaltic Bitumens and Bitumen-Mineral Mixtures", *Journal of the Society of Plastics Engrs.* 11, No. 7

Rijkswaterstaat (1991), Dienst Weg- en Waterbouwkunde, "Guideline Road Engineering Pavement Design" (in Dutch)

SABHA, H., GROENENDIJK J. and MOLENAAR, A.A.A. (1995), "Estimation of crack growth parameters and fatigue characteristics of asphalt mixes using simple tests", Msc. thesis, Delft University of Technology

SALAM Y.M. and MONISMITH C L. (1972), "Fracture Characteristics of Asphalt Concrete", *AAPT.*

SCARPAS, A., BLAAUWENDRAAD J., DE BONDT, A.H. and MOLENAAR, A.A.A. (1993), "CAPA, a Modern Tool for the Analysis of and Design of Pavements", proceedings of the *Second International RILEM conference*

SCARPAS, A., JACOBS, M., VERHOEVEN, K.M. (1994), "Simulation of the crack growth proces in asphalt pavements" (in Dutch), *C.R.O.W publication 82, part I, Wegbouwkundige werkdagen*

SCHMORAK N.S. (1993), "Statistical Analyses for the Verification of the Dutch Design Method for full-depth Pavements" (in Dutch), Msc. thesis, Delfl University of Technology

SHAPERY R.A. (1975), "A Theory of Crack Initiation and Growth in Visco-Elastic Media, part I-IV", *Int. Journal of Fracture,* Volume 11

WEI WANG (1991), "plastic energy damage accumulation theory and its application in fatigue *problem",Proceedings of the Internafional Symposium of Fatigue and Fracfure in Steel and Concrete Structures,* Mardras, India, dec 19-21-1991, page 153–174